Orbit Determination of 1951 Lick

Fengning Ding, Jason Liu, Patrick Rall
Summer Science Program Westmont 2011

Abstract—During the summer of 2011, the asteroid 1951 Lick was observed on seven days using a 14" Meade telescope and a 24" Keck Telescope. From seventeen usable images, the right ascension and declination of the asteroid were measured using least-squares plate reductions. Because the asteroid had just completed a retrograde loop at the time of observation, the rate of change of the range vector was small and difficult to compute. Existing well-developed orbital determination methods such as Gauss-Gibbs's method and Laplace's method are very sensitive to this rate of change, and both methods failed to give accurate orbital parameters. By using Laplace's method to first give reasonably correct estimates and then using five iterations of differential corrections to refine the preliminary results, we were able to compute the orbit of our asteroid. While for most situations, one iteration of differential corrections is enough, the inaccuracy of our initial estimate required multiple iterations to compensate. This method produced spectacular results; relative to an observation made on July 19, the ephemeris calculated from our orbital elements was within 0.112 seconds of the right ascension and 1.56 arcseconds of the declination of the observed coordinates of the asteroid. The orbital elements from our analysis were consistent with previously determined measurements. Our research demonstrates the possibility of computing orbits even in adverse situations and allows the usage of previously unusable data to furnish excellent orbital parameters.

1 Introduction

Due to the potential of some near-earth asteroids to collide with Earth, astronomers are especially interested in the orbits of near-earth asteroids. To ensure accurate monitoring of these hazardous objects, which often move in chaotic orbits perturbed by other planets, astronomers need to repeatedly measure the asteroid's position and velocity with high precision to determine its orbit, which is parametrized by six parameters (corresponding to the six degrees of freedom of the initial conditions): the semimajor axis a, the eccentricity e, the inclination (with respect to the plane of the Earth's orbit) i, the longitude of the ascending node (with respect to the Vernal Equinox) Ω, the argument of the perihelion ω, and the time of the last perihelion passage T_p. These orbital parameters can be used to locate the asteroid in the sky or to generate the position of the asteroid in the future.

In July 2011, as part of the Summer Science Program at Westmont College, we determined the orbit of the asteroid 1951 Lick. We used a 14" telescope and Westmont College's 24" Keck Telescope to take seventeen images on seven different nights to determine the asteroid's right ascension (α) and declination (δ) at specific times. Our seventeen images are augmented by data collected by another team (Hyde, J., Shah, P., and Zhao, M.) observing 1951 Lick.

Because the asteroid was leaving a retrograde loop, the equatorial unit vector $\hat{\rho}$ from the Earth to the asteroid changed very slowly, causing the classical Gauss-Gibbs orbit determination method, which is sensitive to $\frac{d\hat{\rho}}{dt}$, to give nonsensical values. Laplace's method, another classical method of orbit determination, also initially gave inaccurate results. However, since the orbital parameters calculated from Laplace's method were relatively correct, five iterations of differential corrections gave accurate orbital elements for our asteroid. From our computed orbital elements, which are consistent with previous results, we were able to accurately reproduce the ephemeris.

One novel aspect of our work is the application of five iterations of differential corrections. To determine the orbit from most sets of observations, only one iteration is required to refine

the results of either Gauss-Gibbs's method or Laplace's method. However, because of the adverse positions of the Earth and our asteroid in their orbits, Laplace's method gave only a ballpark estimate, so one differential correction did not give adequately accurate orbital elements. We found that repeated iterations of the differential corrections gave a series of orbital parameters that converged to an accurate value. This extended orbital determination method could allow future astronomers to compute orbits of objects in unfavorable circumstances.

2 METHODS

The images used for orbit determination were taken using two telescopes. After median-combining these images into series to reduce noise, a least-squares plate reduction (LSPR) was calculated using star coordinate data from the Naval Observatory Merged Astrometric Dataset (NOMAD) database. These reductions yielded the right ascension, α, and declination, δ, for the asteroid at the observation times. The orbital elements were determined using an implementation of Laplace's method of orbit determination with five iterations of differential corrections.

2.1 Observing and Image Processing

The asteroid was observed on seven days: July 1, July 3, July 8, July 10, July 16, July 19, and July 25 at around 04:00-06:00 UTC First, the approximate apparent α and δ of the asteroid was obtained from NASA's Jet Propulsion Laboratory's HORIZONS (JPL HORIZONS) ephemeris computation service . Software Bisque's TheSkyX software was used to generate a star chart of the region of the sky in which the asteroid would be located. After syncing and focusing the telescope on a nearby star, three or four series of five or seven images were taken with an exposure time of 45 seconds per image. For details see Table 2.

When retrieving the approximate α and δ from JPL HORIZONS, data was collected for the apparent α and δ, which compensates for various systematic errors such as atmospheric distortion. However, our telescope already corrects for these effects, and so the asteroid was always located near the edge of the image. This error was discovered on July 19, and was subsquently corrected for.

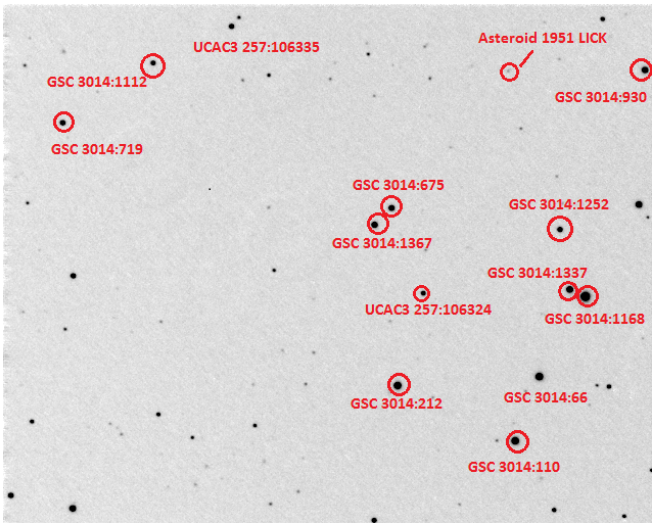

Fig. 1. An example of a combined series of images: Series 2 of the observation on July 10 using the Meade 14" Telescope.

To remove noise and 'hot pixels' (pixels that had been overexposed by a cosmic ray), the images for each series were flat-field corrected, manually aligned, and median combined using Diffraction Limited's MaxIm DL software to form three processed images per observation. The asteroid was identified on the three processed images of each observation by aligning and 'blinking' (changing images over a short time period) the three images. For an example of a processed image see Fig. 1.

2.2 Least-Squares Plate Reduction

Using a Python program written by the authors, the LSPR was calculated for each processed image. The centroids of numerous bright reference stars were obtained using MaxIm DL and compiled in a document along with the stars' α and δ as given by NOMAD. LSPR is a process to find the mapping between the plate x,y coordinates and the equatorial α,δ coordinates that minimizes the least-squares residual. Before LSPR was performed, the effect of different angles of refraction for stars with higher and lower altitude was accounted for. By using the time of observation given by the

Date	Telescope	Sync Star	Filter	# images
July 1	Meade 14″	Omitted due to bad quality		
July 3	DFM 24″	Arcturis	Clear	5
			Clear	5
		Omitted due to bad quality		
July 8	Meade 14″	Images are of wrong part of sky		
		Phecda	Clear	7
			Clear	7
			Clear	7
July 10	Meade 14″	Phecda	Clear	7
			Clear	7
			Clear	7
July 16	Meade 14″	Phecda	V-filter	5
			Clear	5
			Clear	5
			Clear	5
			Clear	5
July 19	Meade 14″	Phecda	Clear	7
			Clear	7
			Clear	7
			Clear	7
July 25	Meade 14″	Phecda	Clear	5
			V-filter	1

TABLE 1
List of series taken in observations

FITS header of each image (and taking into account the difference between our observatory's clock and the US Naval Observatory's clock), the local sidereal time was calculated to convert the equatorial coordinates (from NOMAD) of each reference star into theoretical values for local coordinates of altitude and azimuth. Assuming an index of refraction of $n - 1 = 58.2''$ for the atmosphere, the computed altitude of each star was adjusted to account for the refraction of light by the atmosphere. The adjusted altitude and azimuth were then converted back to theoretical apparent equatorial coordinates.

To find the mapping between the plate x, y coordinates and the equatorial α, δ coordinates by LSPR, we first computed a least-squares linear fit that mapped the x and y plate coordinates of each star to its theoretical apparent equatorial coordinates. Using this mapping, the apparent equatorial coordinates of the center of the image were obtained to calculate the standard ξ and η coordinates for each reference star.[1] Because the standard coordinates are truly linear functions of the plate coordinates, a more accurate least-squares fit was computed that maps the plate coordinates to the standard coordinates. Using this linear transformation, the ξ and η coordinates of the asteroid was obtained, from which the apparent α and δ of the asteroid were calculated. Finally, the apparent equatorial coordinates were transformed back to equatorial coordinates using the same index of refraction of the atmosphere.

To obtain an estimate of the uncertainty of the α and δ of the asteroid, the deviation of the predicted equatorial coordinates of each star and the catalogued coordinates was computed (assuming two degrees of freedom). This residual was possibly due to defects in the CCD chip and telescope mirror, aberration of starlight, inaccurate tabulations of reference star coordinates, or uncertainties in the centroid computations.

2.3 Orbit Determination using Laplace's Method

From the measured α and δ of the asteroid, the classical orbital elements of the asteroid was determined. Because the asteroid had recently exited from a retrograde loop, the asteroid's position relative to earth as a function of time was approximately a straight line, resulting in small values for $\frac{d^2\hat{\rho}}{d\tau^2}$ [2]. The Gauss-Gibbs method of orbit determination[3], which is sensitive to values of $\frac{d^2\hat{\rho}}{d\tau^2}$, produced unrealistic results, and so Laplace's method was used.

We used five observations to obtain $\frac{d\hat{\rho}}{d\tau}$ and $\frac{d^2\hat{\rho}}{d\tau^2}$ for the middle observation. The five unit equatorial vectors are labeled $\hat{\rho}_1$, $\hat{\rho}_2$, $\hat{\rho}_3$, $\hat{\rho}_4$, $\hat{\rho}_5$. The middle range vectors give the position of the asteroid on July 8 and were used to calculate $\frac{d\hat{\rho}}{d\tau}$. The second derivative of $\hat{\rho}$ at the middle observation was computed using $\hat{\rho}_1$, $\hat{\rho}_3$, and $\hat{\rho}_5$, the range vectors of the asteroid on June 27, July 8, and July 25 respectively[4]. This time span was chosen to be large enough for the first derivative to change appreciably.

To compute the first derivative, we used the

1. See [2]

2. τ is the modified time given by $\tau = kt$, for ordinary time t and the Gaussian gravitation constant $k = 0.017....$ All time derivatives in this section are with respect to modified time.

3. Described in [1]

4. The June 27 data was obtained by the other team

second-order Taylor expansion:

$$\begin{aligned}\hat{\rho}_4 &= \hat{\rho}_3 + \hat{\rho}_3'(\tau_4 - \tau_3) + \frac{1}{2}\hat{\rho}_3''(\tau_4 - \tau_3)^2 \\ \hat{\rho}_2 &= \hat{\rho}_3 + \hat{\rho}_3'(\tau_2 - \tau_3) + \frac{1}{2}\hat{\rho}_3''(\tau_2 - \tau_3)^2\end{aligned}$$

from which we solved for $\hat{\rho_3}'$. The second derivative was calculated similarly but with $\hat{\rho}_1$ and $\hat{\rho}_5$ instead of $\hat{\rho}_2$ and $\hat{\rho}_4$. From $\frac{d\hat{\rho}}{d\tau}$ and $\frac{d^2\hat{\rho}}{d\tau^2}$, the standard Laplace method was used to generate the position and velocity vectors of the asteroid[5]. This calculation was done using a Python program.

From the preliminary position and velocity, an ephemeris was generated for the times of each of our observations, and the differences from the measured values, $\Delta\alpha$ and $\Delta\delta$, was calculated. A small change in the position and velocity results in changes of α and δ according to the equations below:

$$\begin{aligned}\Delta\alpha &= \frac{\partial\alpha}{\partial r_x}\Delta r_x + \frac{\partial\alpha}{\partial r_y}\Delta r_y + \frac{\partial\alpha}{\partial r_z}\Delta r_z + \\ &\quad \frac{\partial\alpha}{\partial v_x}\Delta v_x + \frac{\partial\alpha}{\partial v_y}\Delta v_y + \frac{\partial\alpha}{\partial v_z}\Delta v_z \\ \Delta\delta &= \frac{\partial\delta}{\partial r_x}\Delta r_x + \frac{\partial\delta}{\partial r_y}\Delta r_y + \frac{\partial\delta}{\partial r_z}\Delta r_z + \\ &\quad \frac{\partial\delta}{\partial v_x}\Delta v_x + \frac{\partial\delta}{\partial v_y}\Delta v_y + \frac{\partial\delta}{\partial v_z}\Delta v_z\end{aligned}$$

Using six observations of our asteroid, we found least-squares corrections Δr_x, Δr_y, Δr_z, Δv_x, Δv_y, and Δv_z for the position and velocity vectors. Due to inaccurate preliminary position and velocities, these corrected position and velocity vectors were still not accurate (since the differential corrections described above only correct for small inaccuracies), and so this process was iterated five times until the computed orbital elements converged. In each iteration, the last adjusted result for position and velocity was used to calculate new corrections according to the above procedure.

To compute the uncertainties for the orbital elements, we assumed that the α and δ of the asteroid was distributed normally according to the standard deviation computed from the LSPR. A Monte-Carlo method with sample size of five hundred was used to compute the orbital elements using the procedure specified above for a set of asteroid coordinates randomly sampled from the Gaussian distribution. The standard deviation of the computed orbital elements was reported as the uncertainty.

5. See [1]

No. of Corrections	Semimajor Axis	Eccentricity	Inclination
Laplace's Method	1.376	0.0699	39.447
One iteration	1.342	0.0576	38.968
Two iterations	1.384	0.0592	39.078
Three iterations	1.389	0.0604	39.087
Four iterations	1.389	0.0604	39.088
Five iterations	1.389	0.0605	39.088
HORIZONS Value	1.390536	0.0616082	39.08962
No. of Corrections	Ω	ω	T_P
Laplace's Method	129.761	344.711	2455602.859
One iteration	131.535	163.598	2455298.593
Two iterations	130.852	142.718	2455243.991
Three iterations	130.777	140.797	2455238.203
Four iterations	130.773	140.700	2455237.901
Five iterations	130.772	140.695	2455237.885
HORIZONS Value	130.769445	140.4418	2455835.571

TABLE 2
Outputs of Laplace's method and each iteration of differential correction. As the table shows, Laplace's method gave very inaccurate results for ω and T_P. With one iteration of corrections, ω and T_P are much more accurate, but the other orbital elements were over-corrected. Each subsequent iteration improves the value of all orbital elements.

2.4 Photometry

On July 16 and July 25, a V-filter image of the asteroid was taken to measure the V-magnitude of the asteroid. To determine the apparent magnitude of the asteroid, images were taken with a V-Filter in the telescope, instead of the clear filter that was used for astrometry. After taking a series of images with the V-Filter, V-Magnitudes of surrounding stars were obtained from the NOMAD database. From the V-magnitudes of the reference stars, MaximDL computed the V-magnitude of the asteroid.

3 Results

The result of the orbit determination along with the uncertainty are shown in Table 4.

Asteroid V-Mag	Observation	Sync Star VMag
16.861	GSC 2531:1730	12.690
17.122	GSC 2529:1728	12.590

TABLE 3
V-Magnitude of 1951 Lick

a	e	i
1.3894 ± 0.0094 AU	0.06053 ± 0.0024	$39.089 \pm 0.019°$
Ω	ω	T_P
$130.7706 \pm 0.1415°$	$140.65 \pm 3.71°$	2455237.7 ± 11.3 JD

TABLE 4
Measured orbital elements

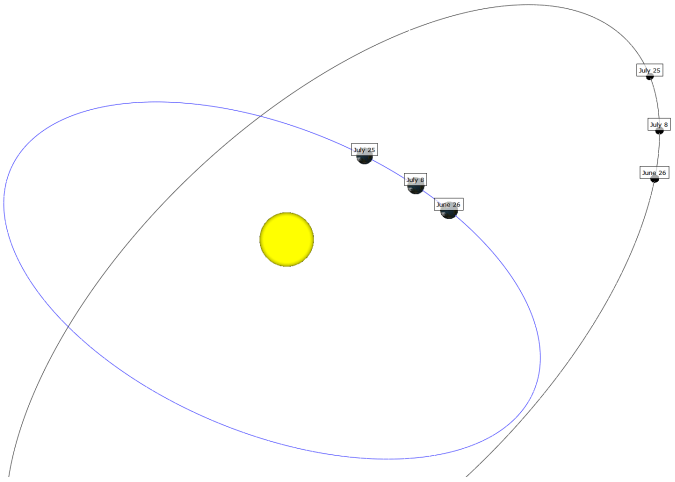

Fig. 2. Position of the asteroid relative to the Earth. The blue loop is that of the Earth's orbit, and the black loop is that of the asteroid. The positions of the earth, going clockwise, are those of July 25th, July 8th, and June 26th; the positions of the asteroid, going clockwise, are those of July 25th, July 8th, and June 26th.

We note that the orbit of the asteroid is similar in eccentricity to that of Mars (with $e = 0.093$[6]) and the point of perihelion is hard to distinguish from other points, so the values for ω and T_p are harder to determine than the other orbital elements.

4 Conclusion

JPL HORIZONS provides values for the orbital elements, which serve as a good comparison to our data. The differences between the orbital elements that were determined in the experimental procedure and those given by JPL are shown in Table 5. The difference between the values is always significantly less than the statistical errors—there are no discrepancies between our orbital elements and that stored in the Horizon database. The ephemerides generated from our orbital elements was also calculated and compared to our observations, as in Table 6. Of course, since orbital elements are constantly changing due to perturbations of the planets, it is irrelevant to compare our orbital elements, which are fitted to best fit the observations (and not the orbit at any precise epoch), and the orbital elements from Horizons, which are given for specific epochs. However, the accuracy of our orbital determination is of theoretical interest, because it demonstrates that accurate orbits can be determined even if Gauss-Gibb's method fails and Laplace's method gives orbital elements that were fairly off due to a non-ideal location of an asteroid with respect to the Earth.

Quantity	Measurement	HORIZONS Value	Difference
a	1.3894 ± 0.0094 AU	1.390536 AU	0.0011 AU
e	0.06053 ± 0.0024	0.0616082	0.0011
i	$39.089 \pm 0.019°$	39.08962°	0.001°
Ω	$130.7706 \pm 0.1415°$	130.769445°	0.0012°
ω	$140.65 \pm 3.71°$	140.4418°	0.21°
T_P	2455237.7 ± 11.3 JD	2455835.571 JD	2.1 JD

TABLE 5
Measured orbital elements in comparison with JPL HORIZONS orbital elements

Date	Observed α	HORIZONS α	Computed α
	Observed δ	HORIZONS δ	Computed δ
Jul 19	12h 24m 7.855s	12h 24m 3.18s	12h 24m 7.667s
	35° 5′ 27.33″	35° 5′ 32.0″	35° 5′ 28.89″

TABLE 6
Comparison of JPL HORIZONS ephemerides and ephemerides from determined orbital elements with observation data

Acknowledgments

The authors would like to thank Dr. Michael Faison, Mr. Martin Mason, and Mary Masterman, Dougal Sutherland, Becky Raph, and

6. See [3]

Sean Mattingly for their help debugging our Python programs, assistance with observations, and teaching us the methodology used in this project.

REFERENCES

[1] Danby, J. M. A. (1962). *Fundamentals of Celestial Mechanics* New York: Macmillan, 1962.
[2] Tatum, J. B. (2002). *Celestial Mechanics* Obtained from M. Mason in 2011
[3] NASA Jet Propulsion Laboratory HORIZONS System. Retrieved from http://ssd.jpl.nasa.gov/?horizons.